Analyst

Ultrafast Surface-Enhanced Raman Spectroscopy

Journal:	*Analyst*
Manuscript ID:	AN-MRV-05-2015-000869
Article Type:	Minireview
Date Submitted by the Author:	01-May-2015
Complete List of Authors:	Keller, Emily; University of Minnesota, Chemistry Brandt, Nathaniel; University of Minnesota, Chemistry Cassabaum, Alyssa; University of Minnesota, Chemistry Frontiera, Renee; University of Minnesota, Chemistry

SCHOLARONE™
Manuscripts

Ultrafast Surface-Enhanced Raman Spectroscopy

Emily L. Keller, Nathaniel C. Brandt, Alyssa A. Cassabaum, Renee R. Frontiera*

Department of Chemistry, University of Minnesota

Minneapolis, MN 55455

*To whom correspondence should be addressed. rrf@umn.edu, 612-624-2501.

Abstract

Ultrafast surface-enhanced Raman spectroscopy (SERS) with pico- and femtosecond time resolution has the ability to elucidate the mechanisms by which plasmons mediate chemical reactions. Here we review three important technological advances in these new methodologies, and discuss their prospects for applications in areas including plasmon-induced chemistry and sensing at very low limits of detection. Surface enhancement, arising from plasmonic materials, has been successfully incorporated with stimulated Raman techniques such as femtosecond stimulated Raman spectroscopy (FSRS) and coherent anti-Stokes Raman spectroscopy (CARS). These techniques are capable of time-resolved measurement on the femtosecond and picosecond time scale and can be used to follow the dynamics of molecules reacting near plasmonic surfaces. We discuss the potential application of ultrafast SERS techniques to probe plasmon-mediated processes, such as H_2 dissociation and solar steam production. Additionally, we discuss the possibilities for high sensitivity SERS sensing using these stimulated Raman spectroscopies.

1. Introduction

The surface-enhanced Raman spectroscopy (SERS) field has matured significantly over the past decades since its discovery,[1, 2] with clear proof of single-molecule sensitivity,[3] a general agreement upon the enhancement mechanism,[4-6] and the development of commercial substrates for SERS applications[7, 8]. More recently, there have been exciting developments in extending SERS techniques and methodologies to the ultrafast regime, in which femtosecond and picosecond time scale techniques have been coupled with the plasmonic materials used for SERS. These successes have opened a new direction in SERS research, in which new methods allow for the direct probing of mechanisms of plasmon-mediated chemical processes.

Plasmon-induced photochemical and photophysical processes have been the recent focus of intense research efforts[9, 10] and convincing demonstrations of these new class of reactions include high efficiency photovoltaics[11-13], water splitting[14, 15], and pollutant degradation[16, 17]. However, many of the recent reports on plasmons as catalysts are phenomenological, as the mechanism of turnover enhancement is unknown and typically behavior is quantified only as an overall improvement in reaction efficiency. The newly developed techniques described in this minireview have great potential in elucidating direct mechanisms of plasmon-induced processes, ideally leading to great improvements in rational device design and overall efficiency.

This paper provides a review of recent ultrafast SERS methods, including surface-enhanced femtosecond stimulated Raman spectroscopy (SE-FSRS), surface-enhanced coherent anti-Stokes Raman spectroscopy (SE-CARS), and time-resolved SE-CARS (TR-SE-CARS). These recently developed techniques have convincingly demonstrated the compatibility of ultrafast pulses with highly enhancing plasmonic substrates, have conclusively proven that

surface enhancement extends to stimulated Raman processes, and have enabled molecular-plasmonic studies on the femtosecond time scale of nuclear motion. These abilities allow one to directly follow bond-making and –breaking processes as plasmons induce new chemical changes in proximal molecular species. Additionally, due to the higher order fields used in stimulated Raman processes, these new techniques may prove to be more sensitive to detection of low concentration analytes as compared to spontaneous SERS processes. These new developments build off of numerous previous works in the field which examined properties including picosecond dynamics,[18, 19] tip enhanced coherent Raman spectroscopy[20], ultrafast decay rates[21], and ultrafast charge-transfer[22].

This paper begins with a discussion of the electromagnetic field enhancement mechanism of SERS, followed by a discussion of the relevant time scales of coupled molecular-plasmonic system dynamics and the advantages of probing these systems with ultrafast spectroscopies. Section 2 discusses three recent demonstrations of ultrafast SERS, consisting of SE-FSRS, SE-CARS, and TR-SE-CARS. These three examples are chosen as they represent some of the most recent advances in the rapidly expanding ultrafast SERS field, and do not include all work in this area. They exemplify significant technical advances, by pushing the limits of time resolution and making measurements of very few numbers of molecules. We follow with an outlook on possible applications of these novel ultrafast SERS techniques, including discussions on plasmon-induced H_2 dissociation, plasmon-driven steam generation, and increased sensing specificity at low concentrations.

1.1. What is a plasmon and how is it related to SERS?

The dramatic signal enhancement characteristic of SERS is due in large part to the enhancement of the electromagnetic fields involved in the Raman measurement by the nanoscale metallic structures typically used as SERS substrates.[4, 23, 24] The underlying origin of the electromagnetic field enhancement lies in the coupling of incident electromagnetic fields to localized surface plasmon resonances (LSPRs) of the nanoscale metallic SERS substrates. In their most basic form, plasmons are oscillations of free electron density relative to fixed nuclei in a metallic lattice and may be excited by light irradiation. Excitation occurs when the applied external oscillating electric field is matched to the resonant plasmon frequency, which is dependent on the dielectric constants of the material employed (Fig. 1a).[25, 26] The transition from bulk plasmon resonance to LSPR occurs as the result of confining the plasmon resonance to a metallic object much smaller than the wavelength of the external electric field, and results in an electric field enhancement near the surface of the metallic object on the order of 10^1 to 10^2.[27]

Fig. 1 shows a to-scale depiction of the creation of the LSPR following light irradiation. In this case, a spherical nanoparticle with radius r is irradiated by light with wavelength λ in the long wavelength limit (given as $r/\lambda<0.1$).[23] The small size of the nanoparticle relative to the wavelength of the irradiating light allows the

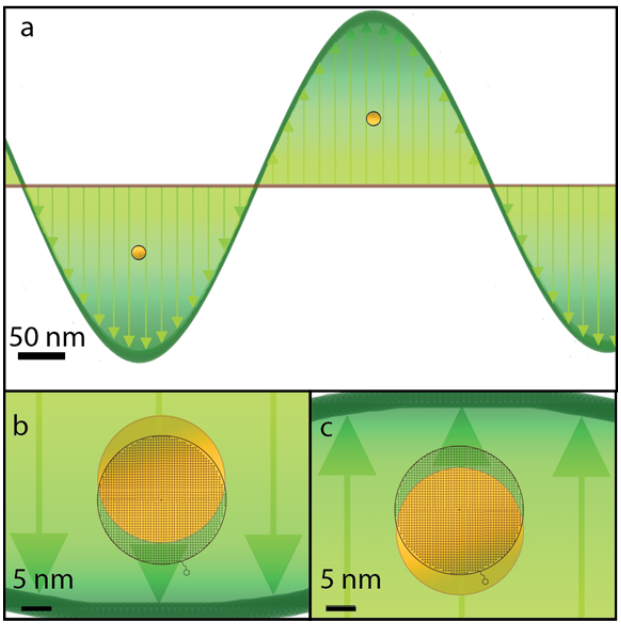

Fig. 1 To-scale depiction of a localized surface plasmon resonance. **a.** Light with a wavelength of approximately 500 nm irradiates a 20 nm gold nanoparticle. Panels **b** and **c** depict the oscillation of the electron cloud (gold) relative to the atomic lattice (grey), in response to the incident electromagnetic field.

electric field surrounding the nanoparticle to be approximated as constant at a given time point. In the case of a sphere, the field enhancement associated with LSPR excitation occurs along the polarization axis of the light and rapidly switches poles at the frequency of the applied field, corresponding to a period of several femtoseconds for visible light (Fig. 1b and 1c).

SERS measurements are typically characterized by an enhancement factor (EF), which quantifies the amount by which the surface increases the Raman signal.[5, 28] In spontaneous Raman-based SERS, the signal enhancement scales as approximately E^4, where E is the electromagnetic field. This can be understood by examining the interactions of the incident and scattered fields with a simple spherical nanoparticle using the formalism given by Van Duyne and colleagues.[23] In this case, the incident field E_0 experiences an enhancement given by:

$$|\mathbf{E}_{\text{out}}|^2 = 2E_0^2|g|^2$$

where $\mathbf{E}_{\text{out}}$ corresponds to the electric field at the surface of the nanoparticle and the field enhancement associated with the nanoparticle is given by the parameter g. The Raman-scattered electromagnetic field will experience a similar enhancement at the Raman-scattered frequency. Comparison of the enhanced fields relative to the incident field E_0 yields the enhancement factor EF as

$$EF = \frac{|\mathbf{E}_{\text{out}}|^2|\mathbf{E}_{\text{out}'}|^2}{|\mathbf{E}_0|^2} = 4|g|^2|g'|^2$$

where the terms corresponding to the Raman-scattered field are denoted by " $'$ ". Assuming the frequency of the Raman-scattered field to be close to the frequency of the incident field yields $g = g'$ and gives an enhancement scaling of g^4. Thus, for a single particle with field

enhancement of 10 (a typical value for an isolated nanosphere), the Raman signal is expected to be enhanced by 10^4.

Stronger electric field enhancement, above that expected for a single metal nanoparticle, can obtained through the use of aggregates of two or more nanoparticles.[27] When two nanostructures are placed close to one another, coupling between the LSPR of each particle results in additional field enhancement in the region between the two particles, which is commonly referred to as a "hot spot". The interaction between the two particles can be considered in a fashion similar to molecular orbital theory in molecular systems, a theory which readily leads to predictions of aggregate plasmon resonance energies and field enhancements.[29, 30] For aggregated particles with field enhancements of 10^4, the SERS EF could be as high as 10^{16}. However, particles and molecules start to break down under these high field strengths and experimental EFs have only been verified to a level of approximately 10^{12}.[5] Additionally, quantum tunneling begins to dominate in this limit, as the nanostructures must be quite close together.[31]

Over the past several decades since its discovery, investigations have focused on the mechanism of SERS signal enhancement and the use of SERS for quantitative sensing of a variety of analytes.[26] The mechanism of enhancement is dominated by the electromagnetic field enhancement described above, with small contributions from chemical processes, such as charge -transfer. In the sensing area, current work focuses on solving long-standing problems such as rigorous quantification of unknown analytes and specificity within complex media. A new and highly active area of SERS research involves the coupling of plasmonic surface enhancement with ultrafast spectroscopies, with the goal of following molecular adsorbate-plasmon interactions on the femtosecond and picosecond time scale. As plasmons have been found to

enhance a number of photochemical and photophysical processes, these new ultrafast methods have the potential to quantify and elucidate the mechanisms behind these new processes, including hot electron and hole transfer, increased heating or scattering, and modification of reactive potential energy surfaces.

1.2. How do plasmons and molecules interact?

In addition to forming the basis for SERS, plasmonic excitations may also be exploited to drive chemical reactions.[32, 33] To most effectively use plasmons to perform chemical reactions, a greater understanding of the decay mechanisms, energy or electron transfer pathways, and the lifetimes of various processes is required. A major goal in the development of new ultrafast SERS methodologies is to quantitatively measure these processes. Here we discuss what is currently known about molecule-plasmon interactions on the ultrafast time scale. In Fig. 2, we depict likely decay pathways for an excited molecular-plasmonic system; however time scales are merely approximate and subject to change for specific systems.

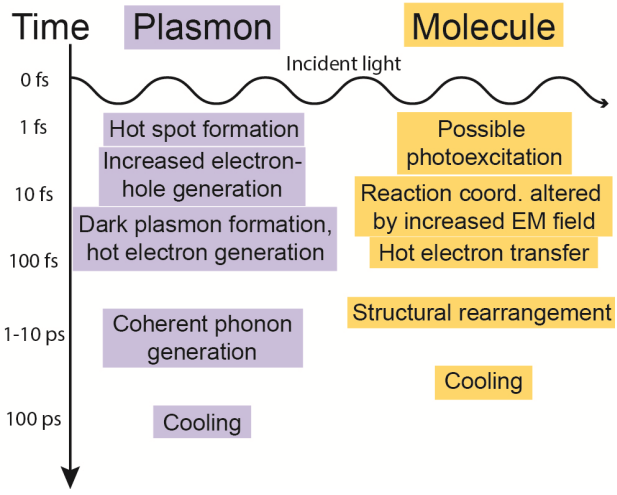

Fig. 2. Approximate time scales of molecular-plasmonic interactions. Timescales are generalized and could vary by several orders of magnitude depending on the system.

Once excited, plasmons quickly decay and dissipate their energy via several pathways (Fig. 2). The decay of the coherent plasmon, which results in the formation of hot electrons, is predicted to occur within approximately 10-100 fs due to electron-electron interactions.[34, 35] Ejected hot electrons could have energies ranging from

the Fermi level to the work function of the plasmonic material and are likely sufficiently energetic to drive chemical reactions in adsorbed analyte molecules.[36, 37] Quantitative measurements of the lifetime and yield of these hot carriers are currently lacking, although numerous theoretical models predict their existence.[36-38] Within the nanoparticle, the initially coherent plasmon gas quickly becomes incoherent, and through interactions between the electrons and the metal phonons, forms a hot metal lattice with a lifetime of 1-10 ps.[39-41] The hot metal lattice then relaxes by coming to equilibrium with the surrounding environment through the release of excess energy as heat over the course of several hundreds of picoseconds to nanoseconds.[42, 43]

Bright, or radiative, plasmons can also decay into dark, or non-radiative, plasmons.[44-48] Dark plasmons exhibit no overall dipole moment, precluding their interaction with plane wave excitation sources. In single nanoparticles, dark plasmons are typically associated with quadrupole or higher multipole modes. In aggregated particles, dark plasmons arise when the individual plasmons associated with single nanoparticle dipoles interact to yield no net dipole moment, creating a dark mode similar to an anti-bonding orbital. Because they cannot be directly excited by incident radiation and experience minimal radiative damping, dark plasmons exhibit longer lifetimes than their bright counterparts. They are also localized in different regions on the nanoparticle and are not visible in extinction spectra or other far-field measurements.[47] Due to their longer lifetimes, dark plasmons have more time to interact with nearby molecules, potentially leading to more efficient plasmon-driven processes. As a result, when formed, dark plasmons are promising avenues of plasmonic research in areas such as plasmon-induced chemistry.

Molecules placed near the hot spots of plasmonic structures may be affected by plasmonic excitations in several ways; however, the precise nature of the interplay between plasmons and nearby molecules is not well understood. Depending on the analyte of interest, the molecule may be photoexcited in the first few femtoseconds after light irradiation independent of the plasmonic excitation. Furthermore, the potential energy surface of a reacting molecule may be rapidly altered due to the intensity of the electric field in these regions, opening the possibility of accessing new reaction coordinates. Additionally, the hot electrons generated on the plasmonic material are transferrable to adsorbed molecules on the femtosecond time scale, which may be used to drive chemical reactions. Due to these plasmonic effects, the molecule could ideally undergo structural rearrangement on the femtosecond and picosecond time scale.

The techniques discussed in Section 2 have the potential to further elucidate plasmonic-molecular interactions, leading to the development of plasmon-mediated chemistry and increased sensing possibilities. Ultrafast Raman spectroscopy forms the common element of all discussed techniques because it allows for the observation of molecular structure through the vibrations of the molecule and changes in structure due to interaction with the plasmon. These structural changes are observed through shifts in the vibrational frequencies of the Raman active modes for a molecule. Ultrafast laser pulses allow for data acquisition on the time scales of the plasmonic and molecular lifetimes, generating “molecular movies” for the course of a reaction. Recently, stimulated Raman techniques have been combined with SERS, increasing the sensitivity of these time-resolved techniques. As a result, LSPR-driven electromagnetic field enhancement can be used to both observe molecular vibrations through SERS as well as drive chemical reactions through hot electron transfer to analyte molecules.

1.3. How does ultrafast spectroscopy probe molecular-plasmonic interactions?

Ultrafast spectroscopies are generally considered to be those which probe systems on the picosecond or femtosecond time scale. Given that molecular vibrational frequencies range from ~100 cm^{-1} to 3000 cm^{-1}, this time scale is comparable to the period of vibrational motion (from 333 fs to 11 fs). Thus, in order to use real-time monitoring of bond-breaking and -making processes induced by plasmons, ultrafast spectroscopies are required.

In this review, we consider ultrafast Raman spectroscopies, due to the strong enhancement of Raman spectroscopy by plasmonic fields, as described above. Time-resolved spontaneous Raman spectroscopy is subject to the time-energy bandwidth product, meaning that there is an inverse relationship between spectral resolution and temporal resolution. In these spectroscopies, time resolution on the order of several picoseconds results in Raman linewidths of tens of cm^{-1}, which is sufficiently fast to observe some but not all of the relevant dynamics.

Stimulated Raman spectroscopies have the ability to extract structural information on time scales shorter than several picoseconds and, in some cases, can provide information on reaction dynamics on the 10s of femtosecond time scale. In this review, we consider two forms of stimulated Raman spectroscopies: femtosecond stimulated Raman spectroscopy (FSRS)[49, 50], and coherent anti-Stokes Raman spectroscopy (CARS)[51, 52]. Both of these spectroscopies involve the interaction of two or three ultrafast laser pulses and vibrational modes in the sample of interest. When coupled with a femtosecond excitation pulse, such as that indicated in Fig. 2, these spectroscopies can be used to monitor chemical change in molecular-plasmonic systems.

2. Novel ultrafast SERS methods to monitor molecular-plasmonic systems

Here we highlight three different ultrafast SERS techniques, which emphasize the range of technical capabilities possible with these methods, including single molecule and time-resolved measurements.

2.1 SE-FSRS

SE-FSRS is a novel spectroscopic technique created by combining FSRS and SERS. FSRS allows for the vibrational dynamics of a system to be monitored over time, creating "molecular movies" of the evolution of the system. A drawback to this technique is that samples need to have high Raman cross sections or be highly concentrated to produce a strong FSRS signal. Adding surface enhancement to the FSRS process provides a significantly more intense spectral signal from fewer molecules, enabling the study of molecular-plasmonic interactions on the femtosecond time scale.

Previous attempts to couple stimulated Raman techniques with the surface enhancing capabilities of plasmonic materials were troubled by issues involving sample degradation. A SE-FSRS experiment by Gilch et. al. convincingly demonstrated that particles aggregated by ionic interactions are not stable under irradiation from high energy, kHz repetition rate femtosecond pulses.[53] In these systems, the particles likely undergo rapid melting or de-aggregation, which surprisingly seems to occur on a time scale faster than vibrational signal generation.

SE-FSRS was demonstrated successfully through the use of higher repetition rate and lower peak power lasers, which enabled the clear generation of SE-FSRS signals with rapid acquisition times. Fig. 3 shows the SERS intensity spectrum of *trans*-1,2-bis(4-pyridyl)-ethylene (BPE) on 100 nm gold nanoparticles encased in silica (red) as well as the SE-FSR spectrum (black).[54] The peaks in the SE-FSR spectrum show dispersive lineshapes where conventional SER spectra show Lorentzian lineshapes. Dispersive lineshapes are not uncommon in stimulated Raman spectroscopies and can also be found when the Raman pump is on resonance with an electronic transition of the system. In this case, the dispersive features result from interactions of the plasmonic nanoparticles and the vibrational coherence used to generate the Raman signal.[55] The SE-FSR spectra show high degrees of spectral (20 cm^{-1}) and temporal (10-100 fs) resolution, and convincingly demonstrate that ultrafast stimulated Raman spectroscopies can be successfully adapted to plasmonically-enhanced nanoscale environments.

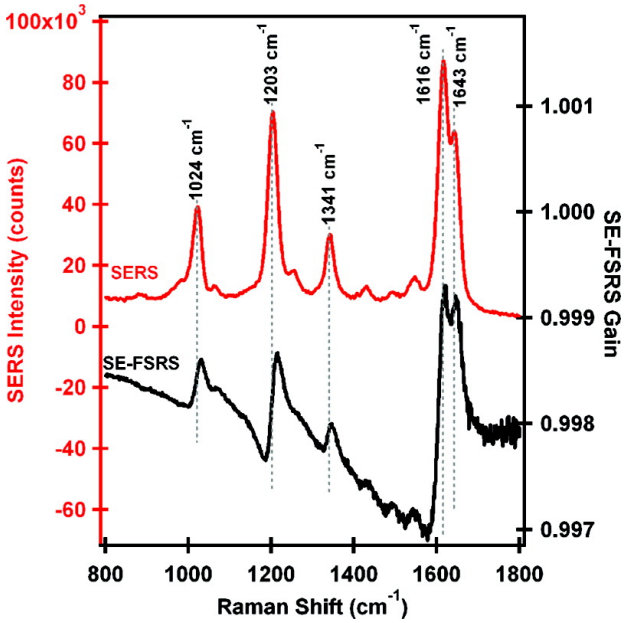

Fig. 3. Proof of principle surface-enhanced femtosecond stimulated Raman spectra. In red is the spontaneous SER spectrum of the bis-pyridyl-ethylene nanoantennas, and in black is the SE-FSR spectrum. The two techniques show isoenergetic features, although the lineshapes are dispersive in SE-FSRS. Figure reproduced with permission from reference [54].

Determining the exact EF of the SE-FSRS process is a crucial factor in the overall sensitivity of this method. As with many SERS EF calculations, the exact determination in this experiment is hindered by uncertainty in the number of molecules participating in the Raman

process. The EF is estimated to be between 10^4-10^6 when assuming a monolayer surface coverage, less than the 10^8 enhancement found in SERS experiments on the same samples.[54, 56] This discrepancy is likely due to particle degradation, as the authors found significant changes in the LSPR over the course of the experiment, demonstrating a change in the plasmonic properties of the material. However, it is clear that high signal-to-noise ratio spectra are easily achievable with this technique.

The clear success of coupling plasmonic materials with femtosecond stimulated Raman techniques forms a first step towards monitoring plasmonically-induced photochemical and photophysical processes. SE-FSRS shows great potential in determining system mechanisms and intermediates that have low signals and short lifetimes that are not able to be detected by other methods, significantly increasing the number of systems and fields of study that can be explored.

2.2. SE-CARS

CARS is a stimulated Raman technique similar to FSRS, which involves the interaction of 2 to 3 laser beams and provides anti-Stokes Raman information in a coherent beam of emitted light. While CARS can suffer from interferences from electronic signals, termed the "non-resonant background", it has been highly useful in imaging and materials characterization.[51] Several attempts have been made to couple the CARS processes with the surface-enhancing capabilities of plasmonic materials, with historical enhancement factors on the order of 10^3.[57, 58]

A more recent experiment by Halas *et al.* demonstrated SE-CARS with single molecule and single particle resolution.[59] This extraordinary sensitivity was achieved with a carefully designed plasmonic substrate consisting of a quadrumer of four Au disks evaporated onto a silica support. Once prepared and characterized, small molecules were introduced to the substrate to determine the EF, which was 10^5 relative to CARS without surface-enhancement. When compared to spontaneous Raman, an EF of 10^{11} was observed. A bi-analyte experiment was performed with p-aminothiophenol (*p*-MA) and adenine, which were used in the previous ensemble measurements, to obtain single molecule data. As bianalyte rather than isotopologue measurements were performed to prove single molecule behavior, the authors of this study did careful surface adsorption measurements to ensure differences in molecular binding affinities did not affect the statistics. As shown in Fig. 4, three different spectra were observed. The spectra either contained peaks associated with only one of the analytes or a combination of peaks from both analytes. With the observed enhancement, the

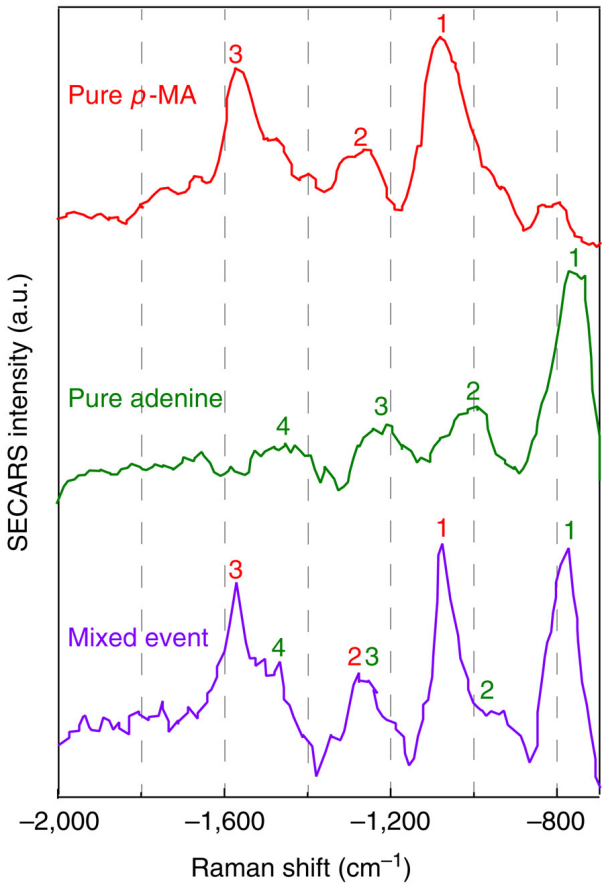

Fig. 4. SE-CAR spectra depicting single molecule detection via the bianalyte method. The top two spectra show each analyte individually and the bottom spectrum is representative of the presence of both analytes. Figure reproduced with permission from reference [59].

Halas group demonstrated the analytical potential of this technique when an appropriately enhancing substrate is used.

2.3. TR-SE-CARS

Both the SE-FSRS and SE-CARS experiments discussed thus far have been ground state measurements, with the undemonstrated potential of coupling these measurements with direct photoexcitation to follow the ultrafast dynamics of the molecular-plasmonic system. The next example, which we term TR-SE-CARS, is a true breakthrough in extracting femtosecond information from a CARS measurement. While not an example of a photoexcited system, femtosecond dynamics corresponding to molecular vibrations were obtained at the single particle and possibly single molecule level.

The recent demonstration of TR-SE-CARS allows for direct observation of molecular vibrations in real time.[60] Measurements of this type were made possible by utilizing the robust sample architecture used in the SE-FSRS experiments described in Section 2.1, in which analyte molecules (BPE, as in the SE-FSRS experiments) were adsorbed to gold nanoparticle dimers and then encapsulated in silica. This allows for SERS signals from single dimer particles to be reliably obtained over long time periods using intense ultrafast laser pulses without significant sample damage. Single particles immobilized on a TEM grid substrate were examined by TR-SE-CARS, in which Raman-active vibrations were excited by a pump pulse pair and then probed at a later time using a single probe pulse (Fig. 5a). Through proper tuning of the frequencies of the pump and Stokes pulses used to generate the TR-SE-CARS signal, the authors were able to excite multiple Raman-active vibrations of BPE. This resulted in a signal that oscillated in time due to the quantum beating of the closely-spaced excited vibrational modes (Fig. 5b). This oscillatory signal appeared on top of a non-resonant background, which likely arose from the

plasmonic response of the nanoparticle structures. While rigorous separation of the plasmonic and molecular responses is not trivial due to the extent of molecule-plasmon coupling being not well understood, the authors were able to extract and analyze the oscillatory features of the spectra.

In addition to forming an important demonstration of femtosecond time-resolved SERS, the authors were able to show evidence that some of the oscillatory TR-SE-CARS signals were suggestive of single molecule behavior through statistical analysis of the dephasing present in each signal. Whereas TR-SE-CARS signals from bulk BPE exhibit rapid dephasing back to zero signal (Fig. 5c), the TR-SE-CARS signals from single dimer particles did not (Fig. 5d). This behavior can be related to the number of molecules generating the signal through analysis of the average signal level at long delay time $\langle S(\tau \to \infty)\rangle$, which can be described by

$$\langle S(\tau \to \infty)\rangle = \frac{1}{NV}$$

where N is the number of particles and V is the number of vibrational states being excited. Through examination of the probability distribution function (PDF) of the amplitude of each signal, with knowledge of V, assignments of N can be made with statistical certainty based on the moment of the signal PDF. As shown in Fig. 5e, simulated TR-SE-CARS signals for one and two molecules show statistically different moments, with $\langle S(\tau \to \infty)\rangle = \frac{1}{2}$ for $N = 1$ and $\langle S(\tau \to \infty)\rangle = \frac{1}{4}$ for $N = 2$. Similar analyses of experimental signals allow for assignment of N, which in some cases confirmed single molecule behavior. It should be noted that single molecule behavior in this case was confirmed only through analyses of TR-SE-CARS traces as opposed to more commonly employed isotopic methods of confirmation, which are challenging under the experimental conditions employed in this work.[61]

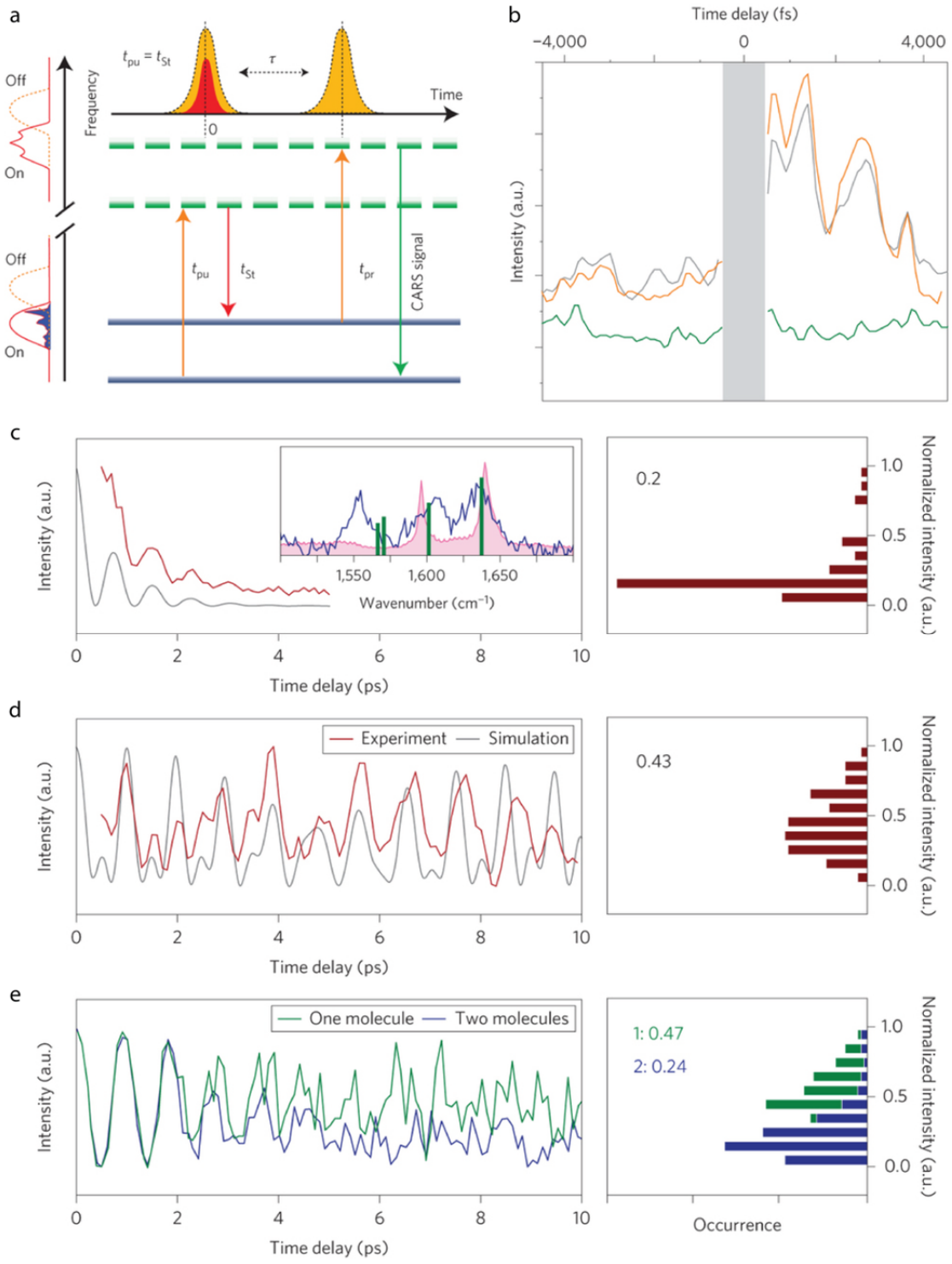

Fig. 5. TR-SE-CARS set-up and spectra **a.** Jabolonski diagram of the pump pair and probe pulses **b.** TR-SE-CAR spectra from SERS-active (orange and gray traces) and non-SERS active (green trace) substrates **c.** damped quantum beating of vibrational modes in bulk BPE obtained by TR-SE-CARS (brown curve) and windowed Fourier transform of bulk BPE Raman signal

(grey curve). The right panel shows the probability distribution function and moment of the brown curve. Inset shows TR-SE-CAR spectrum (blue curve), bulk BPE Raman spectrum (pink curve), and stick spectrum used for simulations **d.** TR-SE-CARS signal from a single dimer (brown curve) compared to simulated signal for stick spectrum in inset of c (grey curve). The PDF and moment of the experimental trace appears in the panel on the right **e.** simulated TR-SE-CARS signals for one molecule (green curve) and two molecules (blue curve). The panel on the right shows PDFs and moments of both traces. Figures reproduced with permission from reference [60].

The combination of SERS with time-resolved measurements, including FSRS and CARS, is needed in order to study plasmon-mediated chemical reactions. The increased signal and resolution offered by the surface-enhanced techniques as well as the ability to collect spectra on the time scale of the reaction allow for the collection of data for unstable intermediates which may not be visible to similar techniques. Additionally, TR-SE-CARS would not only make it possible to study plasmon-mediated reactions as an ensemble but potentially offer the ability to observe how one molecule reacts when it is near a plasmonic hot spot.

3. Future Prospects/Applications

3.1. Plasmonic Processes

The development of the stimulated and time-resolved surface-enhanced Raman methods described above open a new door into the ability to follow plasmon-induced photochemical and photophysical processes in real time. The ability of plasmons to concentrate light, generate highly energetic electrons and holes, and drive new chemical processes is leading to exciting research in coupling these novel methods with various chemical systems. Here we highlight a few of the future possibilities for SE-CARS and SE-FSRS.

3.1.1. H_2 dissociation

Recently, hot electrons generated by exciting plasmonic gold nanoparticles were used to dissociate H_2, which is typically an extremely energetically unfavorable reaction. Plasmon-mediated H_2 dissociation is a light driven reaction, which occurs at ambient conditions.[62, 63] The photocatalytic power of plasmons towards heterogeneous catalysis and energy applications is quite appealing, however there remain significant questions as to the relative roles of hot electrons, light scattering, localized heating, and surface chemistry in these processes.

Determining the mechanism by which plasmon-mediated chemistry occurs is vital towards truly harnessing the power of plasmonic photocatalysts. The proposed mechanism for H_2 dissociation involves sufficiently energetic hot electrons populating an anti-bonding orbital of H_2, resulting in a broken H-H bond. Similarly, D_2 is dissociated and recombines with dissociated H_2 to form HD at a sufficiently high concentration to be quantified with a quadrupole mass spectrometer (QMS).[62] QMS detection allows for the determination of rate constants for this reaction, however it lacks sufficient time resolution and sensitivity to monitor the formation of the unstable intermediates proposed in this mechanism. The time-resolved SERS techniques described above could allow for data acquisition at each point in this photocatalytic process, providing molecular snapshots for each step of the mechanism. The structural information at relevant time scales obtained by time-resolved SERS will show how molecules react near hot spots, providing many new avenues in plasmonic research and applications.

3.1.2. Solar Steam

An additional future application of time-resolved SERS lies in elucidating the mechanism of the recently reported plasmonically-driven steam evolution from liquid water. Irradiation of solutions of nanoparticles in water with focused sunlight has been shown to result in highly

efficient steam generation[64], with promising utility in off-grid applications requiring steam production, such as waste sterilization.[65] This process has been shown to yield steam generation with over 80% energetic efficiency without the need to heat the entire solution volume to its boiling point. The mechanism is believed to entail light trapping by nanoparticles in solution, in which multiple nanoparticle scattering processes followed by nanoparticle absorption results in localization of incident light into a small volume. This yields a compact and nanoscale heat source.[66] However, the temperature rise experienced by the solvent molecules immediately surrounding the nanoparticle and the relative role of collective versus individual nanoparticle heating is still unclear. Additionally, the precise location of vapor nucleation is currently unknown[67], with the shape and spatial distribution of nanoparticles both believed to be important.

Understanding of the precise mechanism of solvent vaporization on nanoparticle surfaces will undoubtedly benefit from the ability of time-resolved SERS to shed light on the ultrafast time scales that govern energy relaxation from nanoparticles into their surroundings. Furthermore, time-resolved SERS can also be exploited to give information on the instantaneous temperature of the solvent immediately surrounding the nanoparticle through comparison of Stokes and anti-Stokes Raman spectra. This would greatly assist in elucidating the precise temperature rise of the solvent layer immediately surrounding the nanoparticle and aid in future design considerations for more efficient solar steam generation.

3.2. Sensing applications

The novel ultrafast SERS methods described in Section 2 have been developed primarily for studies of plasmon-induced photochemical and photophysical processes, but also could have

significant potential for SERS sensing applications. As SE-FSRS and SE-CARS involve coupling stimulated Raman processes with surface enhancement, they have the advantage of coherent signal generation, along with the possibility of field enhancements beyond the E^4 limit as described in Section 1.1.

Stimulated Raman techniques are fundamentally different than the spontaneous Raman techniques traditionally used for SERS. They are two-pulse techniques in which the first pulse induces an upward transition in the molecule from the ground state. The second pulse, which matches the frequency of the Raman shifted photon, stimulates a downward transition. Stimulated Raman therefore increases the probability of Raman scatter compared to spontaneous Raman. Furthermore, the stimulated Raman signal is coherent, meaning it is emitted in a beam-like fashion. This means that every Raman photon can in principle be collected, as opposed to spontaneous Raman signals in which photons are typically scattered in many directions and only a small solid angle is collected. When approaching the limit for single molecule detection, the coherent nature of stimulated Raman scattering may enable greater sensitivity due to greater collection efficiency.

An unexplored area of SERS sensing involves the potentially higher EFs of stimulated Raman spectroscopies as opposed to spontaneous Raman spectroscopies. As discussed in Section 1.1, spontaneous SERS EFs depend roughly on E^4, where E is the applied electromagnetic field. In two and three pulse stimulated Raman spectroscopies, the EF may consist of contributions of multiple enhanced electromagnetic fields. In that case, the SERS EF could, in principle, scale as E^6 or even E^8, in which E represents contributions from the multiple applied electromagnetic fields. This higher order enhancement has yet to be seen experimentally, due to difficulties with sample heterogeneity and breakdown at high fields.. As researchers seek

to sense broad classes of compounds at the single molecule level with SERS, the possible higher order enhancements of stimulated SERS processes, including SE-CARS and SE-FSRS, could represent an exciting path towards greater sensing sensitivity at low concentrations.

4. Conclusion

This review discussed recent developments in ultrafast SERS methodologies, with applications to plasmon-mediated chemical reactions and highly sensitive sensing technologies. We highlighted the need for ultrafast SERS methods by considering the time scales of relevant molecular-plasmonic interactions, with implications for understanding reaction dynamics in numerous light-driven chemical and physical processes. Advances in this area in the past several years have been made by coupling stimulated Raman methods, such as FSRS or CARS, with the surface-enhancing capabilities of plasmonic materials. More recent work has shown the applicability of these techniques to femtosecond time scale measurements, through the demonstration of single molecule TR-SE-CARS. These new techniques open a wide range of systems to study, such as plasmon-mediated H_2 dissociation and solar steam production, as well as opening new avenues for sensing applications. Ultrafast SERS techniques have great potential to further our understanding of plasmonic systems and elucidate mechanisms for plasmon-induced chemical reactions.

5. References

1. D. L. Jeanmaire and R. P. Van Duyne, *J. Electroanal. Chem.*, 1977, **84**, 1-20.
2. M. G. Albrecht and J. A. Creighton, *J. Am. Chem. Soc.*, 1977, **99**, 5215-5217.
3. E. C. Le Ru, M. Meyer and P. G. Etchegoin, *J. Phys. Chem. B*, 2006, **110**, 1944-1948.
4. M. Moskovits, *J. Raman Spectrosc.*, 2005, **36**, 485-496.
5. S. L. Kleinman, R. R. Frontiera, A.-I. Henry, J. A. Dieringer and R. P. Van Duyne, *Phys. Chem. Chem. Phys.*, 2013, **15**, 21-36.
6. L. K. Ausman, S. Li and G. C. Schatz, *J. Phys. Chem. C*, 2012, **116**, 17318-17327.
7. H. Ko, S. Singamaneni and V. V. Tsukruk, *Small*, 2008, **4**, 1576-1599.

8. E. P. Hoppmann, W. W. Yu and I. M. White, *Methods*, 2013, **63**, 219-224.
9. I. Thomann, B. A. Pinaud, Z. Chen, B. M. Clemens, T. F. Jaramillo and M. L. Brongersma, *Nano Lett.*, 2011, **11**, 3440-3446.
10. W. Hou and S. B. Cronin, *Adv. Funct. Mater.*, 2013, **23**, 1612-1619.
11. H. A. Atwater and A. Polman, *Nat. Mater.*, 2010, **9**, 205-213.
12. W. Hou, P. Pavaskar, Z. Liu, J. Theiss, M. Aykol and S. B. Cronin, *Energ. Environ. Sci.*, 2011, **4**, 4650-4655.
13. S. Mubeen, J. Lee, W.-r. Lee, N. Singh, G. D. Stucky and M. Moskovits, *ACS Nano*, 2014, **8**, 6066-6073.
14. Z. W. Liu, Hou, W., Pavaskar, P., Aykol, M., Cronin, S. B., *Nano Lett.*, 2011, **11**, 1111-1116.
15. S. Mubeen, J. Lee, N. Singh, S. Kraemer, G. D. Stucky and M. Moskovits, *Nat. Nanotechnol.*, 2013, **8**, 247-251.
16. W. Hou, Z. Liu, P. Pavaskar, W. H. Hung and S. B. Cronin, *J. Catal.*, 2011, **277**, 149-153.
17. C. Hu, T. Peng, X. Hu, Y. Nie, X. Zhou, J. Qu and H. He, *J. Am. Chem. Soc.*, 2009, **132**, 857-862.
18. J. P. Heritage, J. G. Bergman, A. Pinczuk and J. M. Worlock, *Chem. Phys. Lett.*, 1979, **67**, 229-232.
19. V. Kozich and W. Werncke, *J. Phys. Chem. C*, 2010, **114**, 10484-10488.
20. T. Ichimura, N. Hayazawa, M. Hashimoto, Y. Inouye and S. Kawata, *Phys. Rev. Lett.*, 2004, **92**, 220801.
21. C. M. Galloway, P. G. Etchegoin and E. C. Le Ru, *Phys. Rev. Lett.*, 2009, **103**, 063003.
22. K. Shibamoto, K. Katayama and T. Sawada, *Chem. Phys. Lett.*, 2007, **433**, 385-389.
23. P. L. Stiles, J. A. Dieringer, N. C. Shah and R. P. Van Duyne, *Annu. Rev. Anal. Chem.*, 2008, **1**, 601-626.
24. A. Campion and P. Kambhampati, *Chem. Soc. Rev.*, 1998, **27**, 241-250.
25. K. L. Kelly, E. Coronado, L. L. Zhao and G. C. Schatz, *J. Phys. Chem. B*, 2003, **107**, 668-677.
26. E. C. Le Ru and P. G. Etchegoin, *Principles of surface-enhanced Raman spectroscopy and related plasmonic effects*, Elsevier, Amsterdam, 2009.
27. E. Hao and G. C. Schatz, *J. Chem. Phys.*, 2004, **120**, 357-366.
28. E. C. Le Ru and P. G. Etchegoin, *Annu. Rev. Phys. Chem.*, 2012, **63**, 65-87.
29. P. Nordlander and E. Prodan, *Nano Lett.*, 2004, **4**, 2209-2213.
30. P. K. Jain and M. A. El-Sayed, *Chem. Phys. Lett.*, 2010, **487**, 153-164.
31. W. Zhu and K. B. Crozier, *Nat. Commun.*, 2014, **5**, 5228.
32. L. Brus, *Acc. Chem. Res.*, 2008, **41**, 1742-1749.
33. M. L. Brongersma, N. J. Halas and P. Nordlander, *Nat. Nanotechnol.*, 2015, **10**, 25-34.
34. S. Link and M. A. El-Sayed, *J. Phys. Chem. B*, 1999, **103**, 4212-4217.
35. C. Sönnichsen, T. Franzl, T. Wilk, G. von Plessen, J. Feldmann, O. Wilson and P. Mulvaney, *Phys. Rev. Lett.*, 2002, **88**, 077402.
36. C. Frischkorn and M. Wolf, *Chem. Rev.*, 2006, **106**, 4207-4233.
37. A. Manjavacas, J. G. Liu, V. Kulkarni and P. Nordlander, *ACS Nano*, 2014, **8**, 7630-7638.
38. R. Sundararaman, P. Narang, A. S. Jermyn, W. A. Goddard, III and H. A. Atwater, *Nat. Commun.*, 2014, **5**, 5788.

39. T. S. Ahmadi, S. L. Logunov and M. A. El-Sayed, *J. Phys. Chem.*, 1996, **100**, 8053-8056.
40. J. H. Hodak, A. Henglein and G. V. Hartland, *J. Phys. Chem.*, 2000, **112**, 5942-5947.
41. K. O. Aruda, M. Tagliazucchi, C. M. Sweeney, D. C. Hannah, G. C. Schatz and E. A. Weiss, *P. Natl. Acad. Sci. USA*, 2013, **110**, 4212-4217.
42. K. O. Aruda, M. Tagliazucchi, C. M. Sweeney, D. C. Hannah and E. A. Weiss, *Phys. Chem. Chem. Phys.*, 2013, **15**, 7441-7449.
43. G. V. Hartland, *Phys. Chem. Chem. Phys.*, 2004, **6**, 5263-5274.
44. M. Liu, T.-W. Lee, S. K. Gray, P. Guyot-Sionnest and M. Pelton, *Phys. Rev. Lett.*, 2009, **102**, 107401.
45. D. E. Gómez, Z. Q. Teo, M. Altissimo, T. J. Davis, S. Earl and A. Roberts, *Nano Lett.*, 2013, **13**, 3722-3728.
46. P. Nordlander, *Nat. Nanotechnol.*, 2013, **8**, 76-77.
47. J. B. Herzog, M. W. Knight, Y. Li, K. M. Evans, N. J. Halas and D. Natelson, *Nano Lett.*, 2013, **13**, 1359-1364.
48. S. L. Kleinman, B. Sharma, M. G. Blaber, A.-I. Henry, N. Valley, R. G. Freeman, M. J. Natan, G. C. Schatz and R. P. Van Duyne, *J. Am. Chem. Soc.*, 2012, **135**, 301-308.
49. R. R. Frontiera and R. A. Mathies, *Laser Photonics Rev.*, 2011, **5**, 102-113.
50. P. Kukura, D. W. McCamant and R. A. Mathies, *Annu. Rev. Phys. Chem.*, 2007, **58**, 461-488.
51. J.-X. Cheng and X. S. Xie, *J. Phys. Chem. B*, 2003, **108**, 827-840.
52. D. Oron, N. Dudovich and Y. Silberberg, *Phys. Rev. Lett.*, 2003, **90**, 213902.
53. E. C. Ploetz, M. Gellner, M. Schutz, B. Marx, S. Schlucker and P. Gilch, *Xxii International Conference on Raman Spectroscopy*, **1267**, 88-89.
54. R. R. Frontiera, A.-I. Henry, N. L. Gruenke and R. P. Van Duyne, *J. Phys. Chem. Lett.*, 2011, **2**, 1199-1203.
55. R. R. Frontiera, N. L. Gruenke and R. P. Van Duyne, *Nano Lett.*, 2012, **12**, 5989-5994.
56. K. L. Wustholz, A.-I. Henry, J. M. McMahon, R. G. Freeman, N. Valley, M. E. Piotti, M. J. Natan, G. C. Schatz and R. P. V. Duyne, *J. Am. Chem. Soc.*, 2010, **132**, 10903-10910.
57. E. J. Liang, A. Weippert, J. M. Funk, A. Materny and W. Kiefer, *Chem. Phys. Lett.*, 1994, **227**, 115-120.
58. T. Ichimura, N. Hayazawa, M. Hashimoto, Y. Inouye and S. Kawata, *J. Raman Spectrosc.*, 2003, **34**, 651-654.
59. Y. Zhang, Y.-R. Zhen, O. Neumann, J. K. Day, P. Nordlander and N. J. Halas, *Nat. Commun.*, 2014, **5**, 4424.
60. S. Yampolsky, D. A. Fishman, S. Dey, E. Hulkko, M. Banik, E. O. Potma and V. A. Apkarian, *Nat. Photonics*, 2014, **8**, 650-656.
61. L. Piatkowski, J. T. Hugall and N. F. van Hulst, *Nat. Photonics*, 2014, **8**, 589-591.
62. S. Mukherjee, F. Libisch, N. Large, O. Neumann, L. V. Brown, J. Cheng, J. B. Lassiter, E. A. Carter, P. Nordlander and N. J. Halas, *Nano Lett.*, 2012, **13**, 240-247.
63. S. Mukherjee, L. Zhou, A. M. Goodman, N. Large, C. Ayala-Orozco, Y. Zhang, P. Nordlander and N. J. Halas, *J. Am. Chem. Soc.*, 2013, **136**, 64-67.
64. O. Neumann, A. S. Urban, J. Day, S. Lal, P. Nordlander and N. J. Halas, *ACS Nano*, 2012, **7**, 42-49.
65. O. Neumann, C. Feronti, A. D. Neumann, A. Dong, K. Schell, B. Lu, E. Kim, M. Quinn, S. Thompson, N. Grady, P. Nordlander, M. Oden and N. J. Halas, *P. Natl. Acad. Sci. USA*, 2013, **110**, 11677-11681.

66. N. J. Hogan, A. S. Urban, C. Ayala-Orozco, A. Pimpinelli, P. Nordlander and N. J. Halas, *Nano Lett.*, 2014, **14**, 4640-4645.
67. S. Baral, A. J. Green, M. Y. Livshits, A. O. Govorov and H. H. Richardson, *ACS Nano*, 2014, **8**, 1439-1448.

Table of Contents Image